HHS Public Access

Author manuscript

J Neurophysiol. Author manuscript; available in PMC 2015 September 29.

Published in final edited form as:

J Neurophysiol. 2008 January ; 99(1): 122–132. doi:10.1152/jn.01044.2006.

Modulation of NMDA Receptor Properties and Synaptic Transmission by the NR3A Subunit in Mouse Hippocampal and Cerebrocortical Neurons

Gary Tong[1,2,*], **Hiroto Takahashi**[1,*], **Shichun Tu**[1,*], **Yeonsook Shin**[1,3], **Maria Talantova**[1], **Wagner Zago**[1], **Peng Xia**[1], **Zhiguo Nie**[1], **Thomas Goetz**[1], **Dongxian Zhang**[1], **Stuart A. Lipton**[1,2], and **Nobuki Nakanishi**[1]

[1]Center for Neuroscience, Aging, and Stem Cell Research, Burnham Institute for Medical Research, La Jolla, California

[2]Department of Neurosciences, University of California, San Diego, La Jolla, California

[3]Department of Molecular Pharmacology, Kanazawa University Graduate School of Medicine, Kanazawa, Ishikawa, Japan

Abstract

Expression of the NR3A subunit with NR1/NR2 in *Xenopus* oocytes or mammalian cell lines leads to a reduction in *N*-methyl-D-aspartate (NMDA)-induced currents and decreased Mg^{2+} sensitivity and Ca^{2+} permeability compared with NR1/NR2 receptors. Consistent with these findings, neurons from NR3A knockout (KO) mice exhibit enhanced NMDA-induced currents. Recombinant NR3A can also form excitatory glycine receptors with NR1 in the absence of NR2. However, the effects of NR3A on channel properties in neurons and synaptic transmission have not been fully elucidated. To study physiological roles of NR3A subunits, we generated NR3A transgenic (Tg) mice. Cultured NR3A Tg neurons exhibited two populations of NMDA receptor (NMDAR) channels, reduced Mg^{2+} sensitivity, and decreased Ca^{2+} permeability in response to NMDA/glycine, but glycine alone did not elicit excitatory currents. In addition, NMDAR-mediated excitatory postsynaptic currents (EPSCs) in NR3A Tg hippocampal slices showed reduced Mg^{2+} sensitivity, consistent with the notion that NR3A subunits incorporated into synaptic NMDARs. To study the function of endogenous NR3A subunits, we compared NMDAR-mediated EPSCs in NR3A KO and WT control mice. In NR3A KO mice, the ratio of the amplitudes of the NMDAR-mediated component to α-amino-3-hydroxy-5-methyl-4-isoxazolepropionic acid receptor-mediated component of the EPSC was significantly larger than that seen in WT littermates. This result suggests that NR3A subunits contributed to the NMDAR-mediated component of the EPSC in WT mice. Taken together, these results show that NR3A subunits contribute to NMDAR responses from both synaptic and extra-synaptic receptors, likely composed of NR1, NR2, and NR3 subunits.

Address for reprint requests and other correspondence: G. Tong, Burnham Institute for Medical Research, 10901 N. Torrey Pines Rd., La Jolla, CA 92037 (gtong@burnham.org).

*G. Tong, H. Takahashi, and S. Tu contributed equally to the study.

INTRODUCTION

N-methyl-D-aspartate receptors (NMDARs) play important roles in development, synaptic plasticity, learning and memory, and neurodegeneration (Cull-Candy et al. 2001; Dingledine et al. 1999; Lipton and Rosenberg 1994). Conventional NMDARs require at least two subunits, NR1 and one or more NR2 subunits, to form functional channels (Dingledine et al. 1999; Hollmann and Heinemann 1994). They also require dual agonists, glutamate and glycine, for activation (Anson et al. 1998; Hirai et al. 1996; Kuryatov et al. 1994; Laube et al. 1997). Conventional NMDARs exhibit high Ca^{2+} permeability and voltage-dependent Mg^{2+} blockade. Based on these properties, NMDARs are thought to function as coincident activity detectors (Bliss and Collingridge 1993; Malenka and Nicoll 1999). However, abnormal activation of NMDARs is thought to mediate neuronal degeneration (Rothman and Olney 1987).

We and others have identified a third NMDAR subunit, NR3A (Ciabarra et al. 1995; Das et al. 1998; Sucher et al. 1995). In rodent brains, the level of NR3A protein peaks during the first and second postnatal weeks, gradually decreases, and then persists at a low level into adulthood (Wong et al. 2002). When coexpressed with NR1/NR2 in heterologous expression systems, NR3A decreases the amplitude, Ca^{2+} permeability, and Mg^{2+} sensitivity of NMDA-induced currents and produces a smaller unitary conductance (Chatterton et al. 2002; Ciabarra et al. 1995; Das et al. 1998; Pérez-Otaño et al. 2001; Sasaki et al. 2002; Sucher et al. 1995). Consistent with these findings, the amplitude of NMDA currents in NR3A KO neurons is larger than that of wild-type (WT) neurons. NR3A KO mice also exhibit increased dendritic spine density during early postnatal development (Das et al. 1998) and abnormalities in prepulse inhibition (Brody et al. 2005). Therefore NR3A may play a role in early brain development and modulation of certain behaviors. However, the effects of NR3A on NMDAR properties in neurons and synaptic transmission have not been fully elucidated.

We and others recently cloned a second member of the NR3 family, NR3B (Andersson et al. 2001; Chatterton et al. 2002; Matsuda et al. 2002; Nishi et al. 2001). Like NR3A, NR3B has been reported to decrease whole cell NMDA current amplitude and Ca^{2+} permeability (Matsuda et al. 2003). Surprisingly, NR3A and/or NR3B can form functional channels with NR1 in the absence of NR2 in recombinant expression systems (Chatterton et al. 2002). These channels are activated by glycine alone in the absence of NMDA or glutamate. Whether these glycine-sensitive excitatory channels are functionally present in neurons is not entirely clear.

It has been difficult to isolate channels containing endogenous NR3A in primary neurons for the following two reasons. First, NR3 subunit expression is both temporally and spatially restricted to limited areas of the brain during early developmental stages (Wong et al. 2002). Even at P10, when NR3 expression is at its peak, only a fraction of NR1 and NR2 subunits are associated with NR3 subunits (Al-Hallaq et al. 2002). Second, there are currently no specific pharmacological agonists or antagonists for NR3A subunits. We have therefore generated NR3A Tg and KO mice and used cultured neurons and brain slices from those mice to study effects of NR3A on channel properties and synaptic transmission. Our data

suggest that NR3A subunits alter properties of neuronal NMDARs by forming NR1/NR2/NR3A receptors. Furthermore, endogenous NR3A containing channels appear to contribute to synaptic transmission.

METHODS

Generation of tetracycline-controlled transactivator-NR3A transgenic mice

The transgene vector was constructed by inserting a full-length rat NR3A cDNA into pBI-enhanced green fluorescence protein (EGFP) (BD Biosciences, Palo Alto, CA; see Fig. 1). Functionality of the transgene vector was tested by transfection into human embryonic kidney (HEK) cells constitutively expressing tet-controlled transactivator (tTA). Expression of NR3A and EGFP, assayed by Western blotting and fluorescence microscopy, was specifically induced when doxycycline was removed from the tissue culture medium (data not shown).

The vector was injected into fertilized mouse oocytes to produce Tg mice. Southern blot analysis identified several lines harboring the transgene, and we chose three for further analysis. These mice were genetically crossed with another Tg line carrying a Tg tTA under the control of the calmodulin-dependent kinase type II promoter (CAMKII, Jackson Laboratories, Bar Harbor, ME) (Mansuy et al. 1998). The resulting offspring were genotyped for NR3A and CAMKII, and double-positive Tg mice were further characterized. We selected a single line that expresses the highest level of transgenes in the brain for electrophysiological experiments.

Immunocytochemistry

Under isoflurane anesthesia, adult mice were perfused with phosphate-buffered saline (PBS) followed by 4% paraformaldehyde in PBS. Brains were removed and fixed in 4% paraformaldehyde in PBS at 4°C overnight and then soaked in 30% sucrose in PBS. Brains were embedded in optimal cutting temperature (OCT) compound and sectioned sagittally on a cryostat at a thickness of 20 μm. The sections were air-dried and stored at −20°C when not used immediately. NR3A immunostaining was performed as previously described (Sasaki et al. 2002; Wong et al. 2002).

Western blots

Forebrains from NR3A Tg and WT control mice were dissected and homogenized in 0.32 M sucrose with 10 mM Tris-HCl (pH 7.4). The postsynaptic density fraction (PSD) was prepared as described previously (Das et al. 1998). Electrophoresis was performed using NuPAGE 4–12% BT gels (Invitrogen). Proteins were then transferred onto a nitrocellulose membrane. The antibodies used were polyclonal anti-NR3A (1:1000, Millipore) or monoclonal PSD-95 (1:4000, Millipore), followed by HRP-conjugated anti-rabbit or mouse secondary antibodies (Jackson Laboratories). Proteins were visualized by ECL plus Western Detection Kit (GE Health) on Kodak X-ray film Biomax MR-1 (VWR).

Cell culture

We crossed NR3A/tTA double Tg mice with C57BL/6 mice. The offspring of this cross produced ~25% double positive pups in each litter as expected. We then prepared cultures from the entire litter so that each culture contained both NR3A Tg and WT neurons. Low-density primary hippocampal and cortical cultures were prepared from newborns and maintained in cell culture for 1–3 wk as described previously (Tong and Jahr 1994b). Hippocampi or cortices were enzymatically (papain, Collaborative Research) and mechanically dissociated into a single cell suspension and plated onto glass cover-slips coated with collagen/poly-D-lysine. Neurons expressing the NR3A transgene were identified by concomitant expression of EGFP under fluorescence microscopy.

Brain slice preparations for electrophysiology

Coronal slices of the parietal-occipital cortex or transverse sections of hippocampal slices were obtained using standard methods from littermate mice, either NR3A KO versus WT or NR3A Tg versus WT. In these experiments, WT hippocampal neurons served as a control for the NR3A Tg hippocampal neurons because little NR3A is expressed in the WT hippocampus. Conversely, WT cortical neurons served as a suitable control for the NR3A KO cortical neurons because WT cortex expresses significant levels of NR3A at the ages studied here, particularly in layer V (Wong et al. 2002). Briefly, P10 to P21 animals were anesthetized, decapitated, and brains were quickly removed in oxygenated (95% O_2-5% CO_2), ice-cold artificial cerebrospinal fluid (ACSF). Slices (250–300 μm thick for cortical slices and 300–400 μm thick for hippocampal slices) were prepared with a vibratome (Leica) and immediately transferred into an incubation chamber where a continuous flow of warm (30°C), oxygenated ACSF was supplied to allow recovery. Slices were then placed in ACSF at room temperature for ≥1 h prior to electrophysiological recording. Layer V cortical or hippocampal pyramidal neurons were visualized using an upright infrared-DIC-video-microscope with a ×40 water-immersion objective (Axioskop, Carl Zeiss). Pyramidal neurons were identified by their location, size, shape, and electrophysiological properties (Goetz et al. 1997).

Electrophysiological recordings

For studies of Mg^{2+} sensitivity, Ca^{2+} permeability, and agonist binding affinities of NMDA-induced currents, whole cell recordings were performed on cultured hippocampal neurons with a patch-clamp amplifier (MultiClamp 700A, Axon Instruments, Union City, CA). EGFP-positive (and thus NR3A Tg) and -negative (control, WT) neurons were identified on the same coverslip. The presence of EGFP alone did not affect the properties of NMDA-evoked currents (data not shown). The extracellular recording solution contained (in mM), 150 NaCl, 3 KCl, 10 HEPES, 5 D-glucose, 1–10 $CaCl_2$, 0.02 glycine, 0.03 bicuculline methiodide, 0.01 6-cyano-7-nitroquinoxaline-2,3-dione (CNQX), and 0.001 tetrodotoxin (TTX), adjusted to pH 7.4 with NaOH. The intracellular solution contained (in mM): 128 Cs-gluconate, 9 NaCl, 10 HEPES, 10 EGTA, and 2 $MgCl_2$, adjusted to pH 7.2 with NaOH. NMDA currents were evoked by application of NMDA every 30 s in the presence of glycine.

The Ca^{2+} to monovalent ion permeability ratio (P_{Ca}/P_M) was calculated from the shift in the NMDA-current reversal potential in the presence of 1 mM (E_1, see equation in the following text) and 10 mM (E_2) extracellular Ca^{2+} (Pérez-Otaño et al. 2001; Sasaki et al. 2002). The reversal potentials were obtained by application of NMDA at different holding potentials. An equation derived from the extended Goldman-Hodgkin-Katz equation (assuming $P_K/P_{Na} = 1$) was used to calculate the Ca^{2+} permeability ratio (P_{Ca}/P_M)

$$P_{Ca}/P_M = \frac{M_o(1-\{\exp[2(E_1-E_2)/(RT/F)]\})}{\exp[2(E_1-E_2)/(RT/F)][4Ca_2-4Ca_1]}]$$

where M_o is the extracellular concentration of Na^+ and K^+, E_1 and E_2 are the reversal potentials measured in the presence of 1 and 10 mM extracellular Ca^{2+} concentrations Ca_1 and Ca_2, respectively, R is the universal gas constant, T is absolute temperature, and F is Faraday's constant. Solution changes were made with computer controlled gravity-fed flow tubes (Lester et al. 1993).

Single-channel activity of NMDARs was recorded from outside-out patches of cultured hippocampal neurons [14–22 days in vitro (DIV)]. Patch pipettes were prepared from standard wall borosilicate glass (Warner Instruments) with a final pipette tip resistance in the bath solution ranging from 11 to 14 MΩ. The holding potential was −55 mV after adjusting for the liquid junction potential (5 mV). Patch pipettes contained (in mM) 120 CsCl, 20 tetraethylammonium chloride (TEA-Cl), 10 HEPES, 2.25 EGTA, 1 $CaCl_2$, and 2 $MgCl_2$ (pH 7.4). All recordings were performed in "Ca^{2+}-free" extracellular solution containing (in mM) 170 NaCl, 3 KCl, 5 HEPES, and 50 μM EGTA with no added $CaCl_2$, pH 7.4. For activation of NMDARs, 10 μM NMDA and 20 μM glycine were added to the extracellular solution. Additionally, 30 μM bicuculline, 10 μM CNQX, and 0.5 μM TTX were added to the extracellular solution to block γ-aminobutyric acid (GABA) receptor-, AMPA receptor (AMPAR)-, and Na^+-channel mediated activity, respectively. Recordings were made with an Axopatch 200B patch-clamp amplifier (Axon Instruments-Molecular Devices). Single-channel data were analyzed with the TAC software program (TAC X4.1, Bruxton) as we have previously described (Sasaki et al. 2002).

Synaptic NMDAR responses in slices were assessed using the patch-clamp technique in the whole cell recording configuration. Patch pipettes of 3- to 6-MΩ resistance were filled with a solution containing (in mM) 110 K gluconate, 20 KCl, 2 $MgCl_2$, 10 HEPES, 10 phosphocreatine, 4 ATP, and 0.3 GTP, pH 7.3. Identified neurons were approached with patch pipettes under visual control with positive pressure. GABAergic responses were blocked by addition of 30 μM bicuculline to the bath solution that contained (in mM) 125 NaCl, 25 $NaHCO_3$, 25 glucose, 2.5 KCl, 1.25 NaH_2PO_4, 2 $CaCl_2$, and 1 $MgCl_2$. For cortical slices, EPSCs were evoked by stimulating fibers in layers II/III with a bipolar tungsten electrode connected to a stimulus-isolator unit (WPI, Sarasota, FL; stimulus frequency: 0.1 Hz, current stimulus amplitude ranging from 150 μA to 1.5 mA). AMPAR-mediated EPSCs were measured at a holding potential of −70 mV and further verified by blockade with 20 μM NBQX. To relieve block by extracellular Mg^{2+}, NMDAR-mediated EPSCs were recorded at +40 mV, digitized, and evaluated for amplitude with pCLAMP 9 (Axon

Instruments, Union City, CA) and Origin software (OriginLab, Northampton, MA). To record AMPAR-mediated miniature EPSCs (mEPSCs), Mg^{2+} (1 mM), D-2-amino-5-phosphonovaleric acid (D-APV, 50 μM), and bicuculline (30 μM) were added to the extracellular solution to block NMDAR- and GABAR-mediated spontaneous postsynaptic currents, respectively. In addition, TTX (1μM) was also added to block Na^{+} channels and resulting action currents. All recordings were made at room temperature with a holding potential of −70 mV. The currents were digitally sampled at 10–20 kHz and filtered at 2–5 kHz. Data acquisition and analysis were made with pClamp 9 (Axon Instruments) or a mini analysis program (Synaptosoft, Decatur, GA). Results are expressed as means ± SE. Investigators were blinded to the genotype of the animal during the recording session. For hippocampal slices, the Schaffer collateral afferents in the CA1 region were stimulated in the stratum radiatum within 100 μm of the pyramidal cell layer. All recordings are averages of 5–10 traces unless otherwise stated. Precautions were taken to ensure that the distance from the recording electrode in the cell of interest to the stimulating electrode was approximately equal in all slices.

NR3A KO and WT mice were genotyped as described previously (Das et al. 1998). NR3A Tg mice were identified by expression of EGFP under fluorescence microscopy. All electrophysiology experiments were performed at room temperature.

RESULTS

Generation of tTA-NR3A transgenic mice

To gain further insight into the function of the NR3A subunit, we generated Tg mice overexpressing inducible exogenous NR3A. Figure 1*A* shows the schematic representation of the transgene vector that we constructed. Briefly, the tetracycline (tet) responsive element (TRE) was flanked by a pair of cytomegalovirus (CMV) promoters. NR3A cDNA was placed downstream of one of the CMV promoters (Fig. 1*A*). TRE is activated by the tTA, which is further regulated by exogenous doxycycline. In our experiments, the tet-off system was used, and tTA was kept active by not feeding the mice with doxycycline. The paired CMV promoters drive NR3A in one direction and EGFP in the other, allowing identification of cells expressing the transgenes by fluorescence microscopy (Krestel et al. 2001). Southern blot analysis of Tg mice identified several lines harboring the transgene construct. Three of these lines were mated with another Tg line expressing tTA under the control of the CAMKII promoter (Fig. 1*B*). Using this scheme, NR3A along with EGFP is predicted to be expressed in the same cells that express tTA. We generated three separate Tg mouse lines and examined the expression patterns of transgenes in male mice at 6–8 wk in age. We chose the line presented in Fig. 1*C* for further analysis. In this line, EGFP was expressed in the cerebral cortex, the CA1 region of the hippocampus, and the thalamus.

Figure 1, *D–F*, shows the expression pattern in the hippocampus and cortex of the two transgenes, EGFP, as determined by fluorescence microscopy, and NR3A, observed by immunostaining. The expression pattern of ectopic as opposed to endogenous NR3A was determined by comparing the difference between staining patterns of Tg and non-Tg sibling control mice. As previously reported, at 6–8 wk of age, there is little endogenous NR3A expressed in most areas of the brain (Wong et al. 2002). In Tg mice, both EGFP and NR3A

were prominently expressed in the CA1 pyramidal layer and the dentate gyrus of the hippocampus. Subcellular localization of the two transgene products differ: EGFP was expressed highly in neuronal cell bodies in the CA1 region and dentate gyrus (DG), whereas the Tg NR3A was localized in cell bodies as well as dendrites in CA1 pyramidal neurons. The DG cells and their axons (mossy fibers) were also heavily stained by anti-NR3 antibody. CA2 and CA3 cells expressed relatively low levels of EGFP and NR3A. Figure 1*G* demonstrates the presence of the NR3A subunit in the postsynaptic density fraction (PSD) of forebrain lysates from adult NR3A Tg mice. In contrast, NR3A was not detectable in adult WT control mice, whereas PSD-95, a postsynaptic protein, was equally present in lysates from both mice. This result is consistent with the notion that NR3A protein is localized to postsynaptic sites.

Lack of glycine-evoked excitatory currents in WT and NR3A transgenic neurons

Glycine-evoked excitatory currents have previously been observed in assays using recombinant NR1/NR3 receptors (Chatterton et al. 2002). When we undertook studies looking for similar responses in WT neurons, we did not observe such responses (Fig. 2*B*). One possible reason for this could be the low expression level of endogenous NR3A. Therefore we asked whether these channels were present in NR3A Tg mice.

We prepared hippocampal neurons from Tg and WT mice in a single culture dish as follows. We crossed mice doubly Tg for tTA and NR3A (heterozygous at both loci) with C57BL/6 mice. Hippocampi were dissected from newborn pups of this cross and pooled to generate cultured neurons. Those cultured neurons contained both Tg and WT neurons. Neurons expressing EGFP were identified under epifluorescence microscopy (Fig. 2*A*). Theoretically, the probability of producing a doubly Tg pup in these litters was 25%. In practice, we routinely observed that 10–30% of the neurons in these cultures were EFGP positive after 8–10 DIV. These neurons were also subjected to immunohistochemistry using an anti-NR3 antibody, and all EGFP-positive neurons were strongly NR3 positive (Fig. 2*A*). We considered EGFP-positive neurons as Tg NR3A expressors, whereas EGFP-negative neurons served as internal controls.

Using EGFP as an indicator of exogenous NR3A expression, we asked whether hippocampal NR3A Tg neurons would manifest excitatory glycine responses. In the presence of strychnine, glycine alone failed to induce detectable inward currents in WT (EGFP negative) or NR3A Tg (EGFP positive) neurons (Fig. 2, *B* and *C*). However, application of NMDA and glycine to these neurons induced large inward currents (Fig. 2*B*, $n = 53$) that were blocked by the specific NMDAR antagonist D-APV (50 μM; data not shown). It is possible that NR1/NR3 glycine currents desensitized so fast that they were not detected in the whole cell recording configuration. Thus we attempted to record glycine-sensitive excitatory currents in the outside-out patch configuration with a fast perfusion system [solution exchange time was <1 ms (Tong and Jahr 1994a)]. Again, we failed to detect any glycine-sensitive excitatory currents (Fig. 2*D*, $n = 10$). These results indicate that overexpression of NR3A does not produce functional NR1/NR3 channels that can be detected by patch-clamp methods.

Two types of NMDARs in NR3A transgenic neurons

We next asked whether NMDARs containing NR1/NR2/NR3A subunits could be identified in hippocampal neurons derived from NR3A Tg mice. To do so, we prepared hippocampal cultures from NR3A Tg and WT mice and studied the single-channel properties of NMDAR channels in outside-out patches from NR3A Tg and WT neurons (Fig. 3). Application of NMDA (10 μM) and glycine (20 μM) to outside-out patches from cultured hippocampal NR3A Tg neurons (14–22 DIV) in the nominal absence of extracellular Ca^{2+} evoked two distinct populations of NMDAR channels in all patches. The population of large channels had a conductance of 61 pS, whereas, the population of small channels had a conductance of 40 pS (Fig. 3, *A* and *B*). The large conductance contributed 64.7% of all openings observed in these patches. Analysis of individual openings showed that there were no direct transitions between the large and small conductance levels, suggesting that the small conductance was not a subconductance state (see also Das et al. 1998). The mean open time of the large conductance was 6.9 ms (Fig. 3*C*), whereas that of the small conductance was 6.5 ms (Fig. 3*D*). In contrast, in WT hippocampal neurons, the large conductance (52 pS) represented essentially all of the openings, whereas the small conductance was virtually absent (<3%; Fig. 3, *E* and *F*). The mean open time of the channels in WT patches was 7.1 ms (Fig. 3*G*). These results suggest that overexpression of NR3A subunits in neurons that normally do not express detectable levels of NR3 subunits, such as hippocampal neurons (Wong et al. 2002), induces a small single-channel conductance similar to that previously observed in both recombinant systems and primary neurons expressing NR3A (Das et al. 1998).

Decreased Mg^{2+} sensitivity of NMDARs in NR3A transgenic neurons

We next examined sensitivity to Mg^{2+} blockade of NMDA-induced currents in both NR3A Tg and WT hippocampal neurons. As shown in Fig. 4*A*, application of NMDA (100 μM) with glycine (10 μM) produced inward currents in both NR3A Tg and WT neurons. Concomitant application of Mg^{2+} with NMDA and glycine at a holding potential of −80 mV produced partial blockade of these currents. However, the degree of Mg^{2+} sensitivity was significantly decreased in NR3A Tg neurons compared with WT neurons (Fig. 4*B*). The IC_{50} of Mg^{2+} blockade in WT neurons was 9.9 μM (95% confidence interval: 3.4–28.7 μM), whereas this IC_{50} in NR3A Tg neurons was 133.8 μM (95% confidence interval: 99.0–181.6 μM). There was no significant difference in the Hill coefficient between NR3A Tg and WT neurons (0.61 with 95% confidence interval of 0.22 to 1.01 in WT neurons, 0.97 with 95% confidence interval of 0.70 to 1.25 in NR3A Tg neurons).

We also examined the voltage dependency of Mg^{2+} blockade in these cultured hippocampal neurons. As shown in Fig. 4*C*, in the presence of 100 μM Mg^{2+}, WT cells displayed typical voltage-dependent inhibition of NMDA-induced currents. In contrast, NR3A Tg neurons displayed linear current-voltage (*I–V*) curves in the absence and presence of 100 μM Mg^{2+} (Fig. 4*D*). These results indicate that overexpression of NR3A decreases the voltage-dependent sensitivity of NMDA-evoked currents to Mg^{2+}.

Decreased Ca^{2+} permeability of NR3A transgenic neurons

We determined the relative permeability of Ca^{2+} to monovalent ions flowing through NMDAR channels in cultured NR3A Tg and WT hippocampal neurons. These values were calculated from the shift in reversal potential at two different extracellular Ca^{2+} concentrations (Fig. 5*A*). *I-V* curves were generated from recording traces and the reversal potentials estimated (Fig. 5*B*). In NR3A Tg neurons, the mean shift in reversal potential (E_{shift}) was 7.0 ± 0.9 mV, significantly less than that observed for WT neurons (12.4 ± 1.8 mV, $P < 0.02$ by Student's *t*-test; Fig. 5, *B* and *C*). Ca^{2+} permeability ratios (P_{Ca}/P_M) were derived from the equation presented in METHODS. The relative Ca^{2+} permeability was 3.2 ± 0.5 ($n = 6$) for NR3A Tg neurons, significantly less than that for WT neurons (7.5 ± 1.9, $n = 4$; $P < 0.02$) in agreement with previously published values from cultured hippocampal neurons (Mayer and Westbrook 1987; Skeberdis et al. 2006). Taken together, our findings of two populations of single-channel conductances and decreased Mg^{2+} sensitivity support the notion that at least some NMDARs expressed in NR3A Tg neurons are composed of a combination of NR1, NR2, and NR3A subunits.

Glycine and glutamate potency remain unchanged in NR3A transgenic neurons

Previous studies suggested that glycine binds to NR3A with high affinity (Chatterton et al. 2002; Yao and Mayer 2006). If an NR3A subunit was to replace a glutamate-binding NR2 subunit in a tetrameric NMDAR, we would expect alterations in the glutamate potency or Hill coefficient, for example, in NR3A Tg neurons. We therefore compared the EC_{50} of the concentration-response curves for NMDA and glycine in cultured NR3A Tg and WT hippocampal neurons (Fig. 6). The EC_{50} for NMDA in WT neurons was 15.4 μM (with 95% confidence interval of 12.9–18.4 μM), which was not significantly different from that of NR3A Tg neurons (22.1 μM with 95% confidence interval of 18.2–26.8 μM). In addition, the Hill slope for NMDA was not different between WT (1.87 ± 0.24) and NR3A Tg (1.45 ± 0.16, mean ± SE) neurons (Fig. 6*A*). Furthermore, there was no significant difference in the EC_{50} (0.77 μM with 95% confidence interval of 0.68–0.87 μM for WT; 0.77 μM with 95% confidence interval of 0.67–0.89 μM for NR3A Tg) or the Hill slope (2.05 ± 0.24 for WT and 1.79 ± 0.19 for NR3A Tg) for glycine between WT and NR3A Tg neurons (Fig. 6*B*). These results suggest that over-expression of NR3A subunits in cultured hippocampal neurons had no significant effect on agonist potency.

Reduced Mg^{2+} sensitivity of synaptic NMDARs from NR3A transgenic mice

Our results reported in the preceding text addressed the properties of NMDA-evoked currents in cultured neurons. These currents were mediated by both synaptic and extrasynaptic receptors. We next examined the properties of synaptic NMDAR currents in hippocampal slices prepared from NR3A Tg and WT littermate mice. The genotype of these mice was determined by PCR and verified by EGFP positivity. If the transgenically expressed NR3A subunits were incorporated into synaptic NMDARs, then the Mg^{2+} sensitivity of the NMDAR-mediated component of the EPSC (NMDAR EPSC) might be decreased. To determine if this was indeed the case, NMDAR EPSCs were recorded in the CA1 pyramidal layer, where levels of endogenous NR3A were low (Wong et al. 2002) and transgene expression was prominent (Fig. 1*D*). To minimize potential space-clamp

problems, NMDAR EPSCs were recorded from the proximal dendritic tree. In addition, the stimulating electrode was placed equidistant from the recording electrode in Tg and WT slices. Figure 7, *A* and *B*, shows NMDAR EPSCs recorded in the presence of 1 mM extracellular Mg^{2+} at a holding potential of +40 to −80 mV from WT and NR3A Tg neurons. The Mg^{2+} sensitivity of NMDAR EPSCs was determined by comparing *I–V* curves in the presence of 1 mM extracellular Mg^{2+}. For Tg slices, the amplitude of NMDAR EPSCs (−56.6 ± 8.1 pA, $n = 7$ at a holding potential of −80 mV) was significantly larger than that observed in WT slices (−17.6 ± 4.8 pA, $n = 6$; $P < 0.01$ by Student's *t*-test; Fig. 7*C*). Similar results were also observed at a holding potential of −60 mV (−70.1 ± 19.4 pA, $n = 6$ for Tg neurons; −40.5 ± 11.8 pA, $n = 7$ for WT slices, $P < 0.01$). These results indicate that synaptic NMDAR EPSCs in NR3A Tg slices are less sensitive to voltage-dependent blockade by Mg^{2+} than WT slices. This finding is consistent with the notion that Tg NR3A subunits are incorporated into synaptic NMDARs in the hippocampus.

Increased ratio of the amplitudes of NMDAR EPSCs to AMPAR EPSCs in cortical slices from NR3A KO mice

The foregoing experiments were performed in neurons expressing exogenous NR3A subunits. To study the physiological function of endogenous NR3A subunits, we compared properties of NMDAR EPSCs in WT and NR3A KO mice. Our previous studies revealed an increase in the amplitude of NMDA-evoked currents in acutely dissociated cortical neurons from NR3A KO mice (Das et al. 1998). We argue here that if NR3A subunits are incorporated into synaptic NMDAR channels, we should observe an increase in the NMDAR-mediated component of the EPSC in NR3A KO mice. Because we could not compare the amplitude of NMDAR EPSCs directly, we examined the ratio of the amplitudes of NMDAR EPSCs to AMPAR EPSCs as an indication of the relative magnitude of the NMDAR EPSC response. As discussed in the preceding text, endogenous NR3A is expressed in restricted areas of the brain, particularly in cortical layer V, during a narrow developmental window encompassing the first two postnatal weeks of life (Wong et al. 2002). For this reason, we chose to study NMDAR EPSCs from layer V pyramidal neurons in cortical slices prepared from WT and NR3A KO mice from P10 to P13. NMDAR and AMPAR EPSCs from layer V cortical neurons were evoked by stimulating fibers in layers II/III. The AMPAR EPSC amplitude was calculated from the peak current at a holding potential of −70 mV. The NMDAR EPSC amplitude was calculated by averaging currents obtained ~50 ms after the beginning of the response at a holding potential of +40 mV. Figure 8, *A* and *B*, shows representative traces of NMDAR and AMPAR EPSCs in WT and NR3A KO slices, respectively. The ratio of the amplitudes of NMDAR to AMPAR EPSCs in NR3A KO slices (32.6 ± 2.1, mean ± SE, $n = 8$) was significantly larger than that seen in WT slices (25.7 ±1.5, $n = 11$, $P < 0.05$, Fig. 8*C*).

The change in the amplitude ratio of NMDAR to AMPAR EPSCs could be due to either an increase in NMDAR EPSC amplitude, a decrease in AMPAR EPSC amplitude, or a combination of the two in NR3A KO versus WT mice. To explore this mechanism, we studied the characteristics of miniature EPSCs (mEPSCs) from layer V pyramidal neurons in cortical slices prepared from NR3A and WT mice from P10 to P13 (Fig. 8, *D–G*). Note that the NMDAR-mediated component of the mEPSC was too small to measure accurately in

either preparation. However, we could quantify the AMPAR-mediated component of the mEPSC. Figure 8*D* shows representative traces of AMPAR mEPSCs in WT and NR3A KO slices. We found no significant differences in rise time and decay time constants, mean amplitude (Fig. 8*E*), cumulative probability of amplitude (Fig. 8*F*), or cumulative probability of interevent intervals (Fig. 8*G*) between WT and NR3A KO mice. These findings are consistent with the notion that synaptic NMDAR EPSCs are increased in NR3A KO mice, whereas AMPAR EPSCs remain unchanged and that endogenous NR3A modulates NMDAR-mediated synaptic currents in pyramidal neurons of cortical layer V.

DISCUSSION

NR3A has been hypothesized to act as a dominant interfering molecule of NMDAR activity mediated by NR1 and NR2 subunits. NR3A may also form glycine-sensitive cation channels together with NR1 in the absence of NR2 subunits. These hypotheses were proposed based on studies of NR3 subunits in recombinant expression systems, such as *Xenopus* oocytes, HEK and COS cells (Chatterton et al. 2002; Ciabarra et al. 1995; Pérez-Otaño et al. 2001; Sasaki et al. 2002; Sucher et al. 1995). It has been difficult to isolate channels containing endogenous NR3A in primary neurons for the following two reasons. First, NR3 expression is both temporally and spatially restricted to limited areas of the brain during early developmental stages (Wong et al. 2002). Even at P10, when NR3 expression is at its peak, only a fraction of NR1 and NR2 subunits are associated with NR3 (Al-Hallaq et al. 2002). Second, there are currently no pharmacological agents that act as specific agonists or antagonists on NR3A. To address this situation, we have generated a Tg mouse line overexpressing exogenous NR3A. We then used these mice to undertake functional analyses designed to test the hypotheses cited above.

We first asked whether we could detect NR1/NR3 glycine-responsive channels in hippocampal neurons overexpressing NR3A. Perhaps surprisingly, we did not detect such channels. Several circumstances could account for this finding. First, hippocampal neurons express high levels of endogenous NR1 and NR2 subunits. It is possible that levels of exogenous NR3A are not sufficient to compete with NR1/NR2 interactions, making the formation of NR1/NR3A channels unlikely. This possibility would be particularly favored if NR1 preferentially bound to NR2 rather than to NR3A. Alternatively, NR3A may preferentially bind to NR2 rather than to NR1. Thus NR3A may be more frequently incorporated into NR1/NR2/NR3 channels rather than into NR1/NR3 channels. Second, the formation of NR1/NR3 channels may be specific to the expression system used to assay such channels. For example, we cannot rule out the possibility that *Xenopus* oocytes express accessory molecule(s) contributing to the formation of NR1/NR3 channels. Such factors may be a part of the NR1/NR3 channel complex or alternatively could be required for the surface expression of NR1/NR3 channels. However, we (Talantova and Lipton, unpublished observations) and our colleagues (Piña-Crespo and Heinemann 2004) as well as Smothers and Woodward (2007) recently found that excitatory glycine cation channels are also formed in HEK 293 cells expressing NR1 and NR3 subunits. Therefore such accessory molecule(s) would have to also be present in mammalian cell types other than primary neurons. Third, NR1/NR3 channels could possibly be localized in presynaptic terminals of neurons. If this is the case, we might not detect excitatory glycine currents in whole cell

recordings from the soma. However, our previous immuno-electron microscopy study revealed only postsynaptic NR3 protein (Wong et al. 2002).

Here we show that overexpression of NR3A in hippocampal neurons alters the properties of NMDA-induced currents. Compared with native (NR1/NR2) NMDARs, channels in these neurons exhibit an additional smaller conductance with less sensitivity to Mg^{2+} blockade and less permeability to Ca^{2+}. Based on these findings, we propose that NR3A is most likely incorporated into NR1/NR2 receptor complexes to form NR1/NR2/NR3 neuronal channels. This overall conclusion is based on the following observations. First, NR3A overexpression significantly alters channel properties. Second, NR2 is likely to be part of a channel complex because it contains the glutamate/NMDA-binding domain (NMDA must be present for channel activation). Third, NR1 is likely to be part of the complex because surface expression of both NR2 and NR3 subunits requires their association with NR1 in the endoplasmic reticulum (Fukaya et al. 2003; McIlhinney et al. 1998; Pérez-Otaño et al. 2001; Standley et al. 2000). Our results also suggest that NR3A acts as a dominant-interfering molecule of NMDAR activity when it is a part of NR1/NR2/NR3 channels. Specifically, channels composed of NR1/NR2/NR3 subunits had a smaller unitary conductance and somewhat increased mean open time compared with NR1/NR2 channels. In addition, Ca^{2+} influx through the NMDAR-associated channels is a crucial property distinguishing the NMDAR from non-NMDA/glutamate receptor activity. Similarly, voltage-dependent Mg^{2+} blockade is thought to be crucial to the function of the NMDAR as a coincidence detector of activity (Bliss and Collingridge 1993; Malenka and Nicoll 1999). Findings reported here indicate that inclusion of NR3A into NR1/NR2 receptors significantly reduces Ca^{2+} permeability and Mg^{2+} sensitivity, resulting a similarity to non-NMDA channels. Finally, we propose that addition of NR3A into functional NMDAR receptors increases the complexity of the channel properties. It has been shown previously that alternative splicing of NR1 as well as variation among NR2 subunits can create diversity in channel properties, including Ca^{2+} permeability, Mg^{2+} sensitivity, and decay time constants (Kew et al. 1998; Kirson and Yaari 2000; Kirson et al. 1999; Paudice et al. 1998; Rumbaugh and Vicini 1999; Tovar and Westbrook 1999). Our findings suggest that we should also consider NR3A as a potential factor in modulating these channel properties. In fact, some studies predicting the presence of specific NR1 splice variants or NR2 subunits based on altered channel properties may require reinterpretation if NR3 subunits were also present.

In the present study, we did not observe a significant change in NMDA or glycine potency in neurons overexpressing NR3A subunits. Previous studies using both eletrophysiological and biochemical assays, however, suggest that glycine binds to NR3 subunits (Chatterton et al. 2002; Yao and Mayer 2006). Several possibilities may account for this finding. NR3A may replace one NR1 subunit and form neuronal tetrameric NMDAR-associated channels composed of one NR1, one NR3, and two NR2 subunits. Alternatively, NR3 may act as a regulatory subunit that does not contribute to glycine binding in triplet subunit (NR1/NR2/NR3) channels (Villmann et al. 1999). Additionally, because NR3A Tg neurons contain at least two different types of NMDAR channels, namely, conventional channels composed of NR1/NR2 subunits and triplet subunit channels, it is possible that small changes in agonist potency may not be reflected in the observed dose-response curves and thus in the measured agonist potency.

Our new studies using slice preparations confirm the notion that NR3A subunits are incorporated into endogenous synaptic NMDARs (Pérez-Otaño et al. 2006). First, overexpression of NR3A reduced Mg^{2+} sensitivity of NMDAR EPSCs recorded in hippocampal slices. The reduction in Mg^{2+} sensitivity of NMDAR EPSCs in slices from NR3A Tg mice is also consistent with our results in cultured neurons. Second, cortical neurons in slice preparations from NR3A KO mice displayed an increased amplitude of NMDAR EPSCs, suggesting that endogenous NR3A affected these responses in WT mice.

The finding that NR3A subunits contribute to and modify synaptic transmission strengthens the notion that this molecule may be involved in early development and synaptic plasticity (Das et al. 1998). We recently found that NR3A KO mice manifest enhanced prepulse inhibition (PPI), an operational measure of sensorimotor gating, which is impaired in conditions such as schizophrenia and attention deficit disorder with hyperactivity (Brody et al. 2005). Effects on synaptic NMDARs may underlie the abnormal PPI seen in NR3A KO mice because NMDAR activity is known to affect changes in PPI (Geyer et al. 2001). Similarly, NR3A may play a role in the pathophysiology of neurodegeneration mediated by excessive NMDAR activity (Lipton and Rosenberg 1994). In this case, NR3A could act as a neuroprotective molecule because it decreases the amplitude of the unitary conductance of NMDAR-operated channels and limits excessive Ca^{2+} influx by decreasing Ca^{2+} permeability, making it a potential reagent in a strategy to combat neurodegeneration.

Acknowledgments

We thank C. Funamoto and T. Hong Fang for excellent technical support. Present addresses: H. Takahashi, Janelia Farm Research Campus, Howard Hughes Medical Institute (HHMI), 19700 Helix Dr, Ashburn, VA 201476; and T. Goetz, Klinik für Psychiatrie und Psychotherapie, Universitätsklinikum Carl Gustav Carus Dresden, Technische Universität Dresden, Fetscherstr. 74, 01307 Dresden, Germany.

GRANTS

This work was supported by National Institute of Health Grants P01 HD-29587 to S. A. Lipton, N. Nakanishi, D. Zago, and G. Tong, R01 EY-05477 to S. A. Lipton, R01 MH-53535 to N. Nakanishi, and K12 AG-00975 to G. Tong and a postdoctoral scholarship from the Deutsche Forschungsgemeinschaft to T. Goetz.

References

Al-Hallaq RA, Jarabek BR, Fu Z, Vicini S, Wolfe BB, Yasuda RP. Association of NR3A with the *N*-methyl-D-aspartate receptor NR1 and NR2 subunits. Mol Pharmacol. 2002; 62:1119–1127. [PubMed: 12391275]

Andersson O, Stenqvist A, Attersand A, von Euler G. Nucleotide sequence, genomic organization, and chromosomal localization of genes encoding the human NMDA receptor subunits NR3A and NR3B. Genomics. 2001; 78:178–184. [PubMed: 11735224]

Anson LC, Chen PE, Wyllie DJ, Colquhoun D, Schoepfer R. Identification of amino acid residues of the NR2A subunit that control glutamate potency in recombinant NR1/NR2A NMDA receptors. J Neurosci. 1998; 18:581–589. [PubMed: 9425000]

Bliss TVP, Collingridge GL. A synaptic model of memory: long-term potentiation in the hippocampus. Nature. 1993; 361:31–39. [PubMed: 8421494]

Brody SA, Nakanishi N, Tu S, Lipton SA, Geyer MA. A developmental influence of the *N*-methyl-D-aspartate receptor NR3A subunit on prepulse inhibition of startle. Bioll Psychiatry. 2005; 57:1147–1152.

Chatterton JE, Awobuluyi M, Premkumar LS, Takahashi H, Talantova M, Shin Y, Cui J, Tu S, Sevarino KA, Nakanishi N, Tong G, Lipton SA, Zhang D. Excitatory glycine receptors containing the NR3 family of NMDA receptor subunits. Nature. 2002; 415:793–798. [PubMed: 11823786]

Ciabarra AM, Sullivan JM, Gahn LG, Pecht G, Heinemann S, Sevarino KA. Cloning and characterization of chi-1: a developmentally regulated member of a novel class of the ionotropic glutamate receptor family. J Neurosci. 1995; 15:6498–6508. [PubMed: 7472412]

Cull-Candy S, Brickley S, Farrant M. NMDA receptor subunits: diversity, development and disease. Curr Opin Neurobio. 2001; 11:327–335.

Das S, Sasaki YF, Rothe T, Premkumar LS, Takasu M, Crandall JE, Dikkes P, Conner DA, Rayudu PV, Cheung W, Chen HS, Lipton SA, Nakanishi N. Increased NMDA current and spine density in mice lacking the NMDA receptor subunit NR3A. Nature. 1998; 393:377–381. [PubMed: 9620802]

Dingledine R, Borges K, Bowie D, Traynelis SF. The glutamate receptor ion channels. Pharmacol Rev. 1999; 51:7–61. [PubMed: 10049997]

Fukaya M, Kato A, Lovett C, Tonegawa S, Watanabe M. Retention of NMDA receptor NR2 subunits in the lumen of endoplasmic reticulum in targeted NR1 knockout mice. Proc Natl Acad Sci USA. 2003; 100:4855–4860. [PubMed: 12676993]

Geyer MA, Krebs-Thomson K, Braff DL, Swerdlow NR. Pharmacological studies of prepulse inhibition models of sensorimotor gating deficits in schizophrenia: a decade in review. Psychopharmacology. 2001; 156:117–154. [PubMed: 11549216]

Goetz T, Kraushaar U, Geiger J, Lubke J, Berger T, Jonas P. Functional properties of AMPA and NMDA receptors expressed in identified types of basal ganglia neurons. J Neurosci. 1997; 17:204–215. [PubMed: 8987749]

Hirai H, Kirsch J, Laube B, Betz H, Kuhse J. The glycine binding site of the *N*-methyl-D-aspartate receptor subunit NR1: identification of novel determinants of co-agonist potentiation in the extracellular M3–M4 loop region. Proc Natl Acad Sci USA. 1996; 93:6031–6036. [PubMed: 8650214]

Hollmann M, Heinemann S. Cloned glutamate receptors. Annu Rev Neurosci. 1994; 17:31–108. [PubMed: 8210177]

Kew JNC, Richards JG, Mutel V, Kemp JA. Developmental changes in NMDA receptor glycine affinity and ifenprodil sensitivity reveal three distinct populations of NMDA receptors in individual rat cortical neurons. J Neurosci. 1998; 18:1935–1943. [PubMed: 9482779]

Kirson ED, Schirra C, Konnerth A, Yaari Y. Early postnatal switch in magnesium sensitivity of NMDA receptors in rat CA1 pyramidal cells. J Physiol. 1999; 521:99–111. [PubMed: 10562337]

Kirson ED, Yaari Y. Unique properties of NMDA receptors enhance synaptic excitation of radiatum giant cells in rat hippocampus. J Neurosci. 2000; 20:4844–4854. [PubMed: 10864941]

Krestel HE, Mayford M, Seeburg PH, Sprengel R. A GFP-equipped bidirectional expression module well suited for monitoring tetracycline-regulated gene expression in mouse. Nucleic Acids Res. 2001; 29:E39. [PubMed: 11266574]

Kuryatov A, Laube B, Betz H, Kuhse J. Mutational analysis of the glycine-binding site of the NMDA receptor: structural similarity with bacterial amino acid-binding proteins. Neuron. 1994; 12:1291–1300. [PubMed: 8011339]

Laube B, Hirai H, Sturgess M, Betz H, Kuhse J. Molecular determinants of agonist discrimination by NMDA receptor subunits: analysis of the glutamate binding site on the NR2B subunit. Neuron. 1997; 18:493–503. [PubMed: 9115742]

Lester RA, Tong G, Jahr CE. Interactions between the glycine and glutamate binding sites of the NMDA receptor. J Neurosci. 1993; 13:1088–1096. [PubMed: 8095067]

Lipton SA, Rosenberg PA. Excitatory amino acids as a final common pathway for neurologic disorders. N Engl J Med. 1994; 330:613–622. [PubMed: 7905600]

Malenka RC, Nicoll RA. Long-term potentiation—a decade of progress? Science. 1999; 285:1870–1874. [PubMed: 10489359]

Mansuy IM, Winder DG, Moallem TM, Osman M, Mayford M, Hawkins RD, Kandel ER. Inducible and reversible gene expression with the rtTA system for the study of memory. Neuron. 1998; 21:257–265. [PubMed: 9728905]

Matsuda K, Fletcher M, Kamiya Y, Yuzaki M. Specific assembly with the NMDA receptor 3B subunit controls surface expression and calcium permeability of NMDA receptors. J Neurosci. 2003; 23:10064–10073. [PubMed: 14602821]

Matsuda K, Kamiya Y, Matsuda S, Yuzaki M. Cloning and characterization of a novel NMDA receptor subunit NR3B: a dominant subunit that reduces calcium permeability. Brain Res Mol Brain Res. 2002; 100:43–52. [PubMed: 12008020]

Mayer ML, Westbrook GL. Permeation and block of *N*-methyl-D-aspartic acid receptor channels by divalent cations in mouse cultured central neurons. J Physiol. 1987; 394:501–527. [PubMed: 2451020]

McIlhinney RA, Le Bourdelles B, Molnar E, Tricaud N, Streit P, Whiting PJ. Assembly intracellular targeting and cell surface expression of the human *N*-methyl-D-aspartate receptor subunits NR1a and NR2A in transfected cells. Neuropharmacol. 1998; 37:1355–1367.

Nishi M, Hinds H, Lu H-P, Kawata M, Hayashi Y. Motoneuron-specific expression of NR3B, a novel NMDA-type glutamate receptor subunit that works in a dominant-negative manner. J Neurosci. 2001; 21:RC185. [PubMed: 11717388]

Paudice P, Gemignani A, Raiteri M. Evidence for functional native NMDA receptors activated by glycine or D-serine alone in the absence of glutamatergic coagonist. Eur J Neurosci. 1998; 10:2934–2944. [PubMed: 9758163]

Pérez-Otaño I, Lujan R, Tavalin SJ, Plomann M, Modregger J, Liu X-B, Jones EG, Heinemann SF, Lo DC, Ehlers MD. Endocytosis and synaptic removal of NR3A-containing NMDA receptors by PACSIN1/syndapin1. Nat Neurosci. 2006; 9:611–621. [PubMed: 16617342]

Pérez-Otaño I, Schulteis CT, Contractor A, Lipton SA, Trimmer JS, Sucher NJ, Heinemann SF. Assembly with the NR1 subunit is required for surface expression of NR3A-containing NMDA receptors. J Neurosci. 2001; 21:1228–1237. [PubMed: 11160393]

Piña-Crespo JC, Heinemann SF. Physioloogical and pharmacological properties of recombinant NR3-type receptors expressed in mammalian cells. Soc Neurosci Abstr. 2004:957.1.

Rothman SM, Olney JW. Excitotoxicity and the NMDA receptor. Trends Neurosci. 1987; 10:299–302.

Rumbaugh G, Vicini S. Distinct synaptic and extrasynaptic NMDA receptors in developing cerebellar granule neurons. J Neurosci. 1999; 19:10603–10610. [PubMed: 10594044]

Sasaki YF, Rothe T, Premkumar LS, Das S, Cui J, Talantova MV, Wong H-K, Gong X, Chan SF, Zhang D, Nakanishi N, Sucher NJ, Lipton SA. Characterization and comparison of the NR3A subunit of the NMDA receptor in recombinant systems and primary cortical neurons. J Neurophysiol. 2002; 87:2052–2063.

Skeberdis VA, Chevaleyre V, Lau CG, Goldberg JH, Pettit DL, Suadicani SO, Lin Y, Bennett MVL, Yuste R, Castillo PE, Zukin RS. Protein kinase A regulates calcium permeability of NMDA receptors. Nat Neurosci. 2006; 9:501–510. [PubMed: 16531999]

Smothers CT, Woodward JJ. Pharmacological characterization of glycine-activated currents in HEK 293 cells expressing *N*-methyl-D-aspartate NR1 and NR3 subunits. J Pharmacol Exp Ther. 2007; 322:739–748. [PubMed: 17502428]

Standley S, Roche KW, McCallum J, Sans N, Wenthold RJ. PDZ domain suppression of an ER retention signal in NMDA receptor NR1 splice variants. Neuron. 2000; 28:887–898. [PubMed: 11163274]

Sucher NJ, Akbarian S, Chi CL, Leclerc CL, Awobuluyi M, Deitcher DL, Wu MK, Yuan JP, Jones EG, Lipton SA. Developmental and regional expression pattern of a novel NMDA receptor-like subunit (NMDAR-L) in the rodent brain. J Neurosci. 1995; 15:6509–6520. [PubMed: 7472413]

Tong G, Jahr CE. Block of glutamate transporters potentiates postsynaptic excitation. Neuron. 1994a; 13:1195–1203. [PubMed: 7946356]

Tong G, Jahr CE. Multivesicular release from excitatory synapses of cultured hippocampal neurons. Neuron. 1994b; 12:51–59. [PubMed: 7507341]

Tovar KR, Westbrook GL. The incorporation of NMDA receptors with a distinct subunit composition at nascent hippocampal synapses in vitro. J Neurosci. 1999; 19:4180–4188. [PubMed: 10234045]

Villmann C, Strutz N, Morth T, Hollmann M. Investigation by ion channel domain transplantation of rat glutamate receptor subunits, orphan receptors and a putative NMDA receptor subunit. Eur J Neurosci. 1999; 11:1765–1778. [PubMed: 10215929]

Wong HK, Liu XB, Matos MF, Chan SF, Pérez-Otaño I, Boysen M, Cui J, Nakanishi N, Trimmer JS, Jones EG, Lipton SA, Sucher NJ. Temporal and regional expression of NMDA receptor subunit NR3A in the mammalian brain. J Comp Neurol. 2002; 450:303–317. [PubMed: 12209845]

Yao Y, Mayer ML. Characterization of a soluble ligand binding domain of the NMDA receptor regulatory subunit NR3A. J Neurosci. 2006; 26:4559–4566. [PubMed: 16641235]

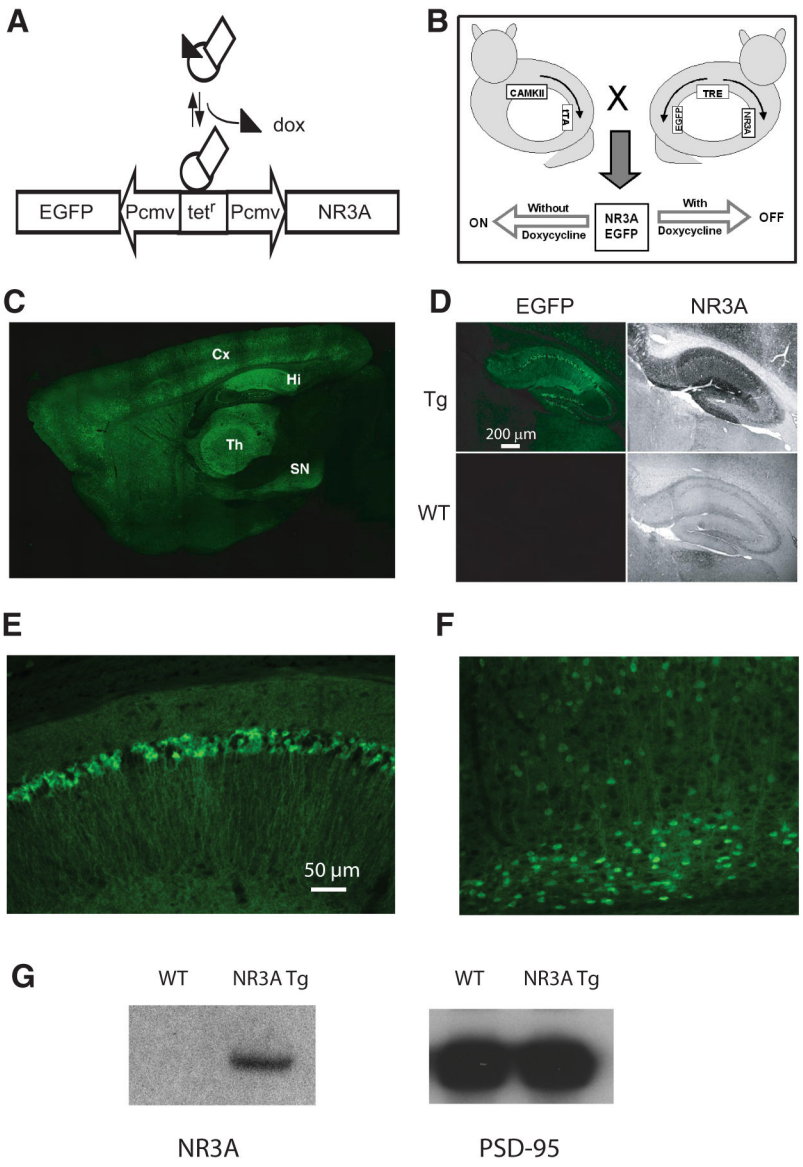

FIG. 1.

Generation of NR3A transgenic (Tg) mice and expression of transgenes. *A*: schematic representation of the transgene vector. The tetracycline-responsive (tet^r) element is flanked by a pair of cytomegalovirus (CMV) promoters (Pcmv) that direct gene expression in opposite directions. tet^r is regulated by tet-controlled transactivator (tTA, represented by a combination of a rectangle and an oval), which is encoded on a separate transgene. The type of tTA used here activates tet^r in the absence of doxycycline (a tetracycline derivative; dox); dox, in turn, suppresses tTA activity. *B*: schematic representation of the generation of NR3A Tg mice. Two Tg lines, 1 carrying tTA under the CamKII promoter and the other carrying the NR3A and enhanced green fluorescence protein (EGFP) transgenes under the tet-responsive element (TRE), were crossed to generate double Tg mice. In these mice, transcription of Tg NR3A and EGFP can be repressed by doxycycline. *C*: strong EGFP expression was observed in the cerebral cortex (Cx), hippocampus (Hi), thalamus (Th), and

substantia nigra (SN). Weak EGFP expression was seen in other parts of the brain. *D*: expression of transgenes for EGFP and NR3A in the hippocampus. Epifluorescence microscopy was performed on a Tg mouse (*top left*) and a control littermate (*bottom left*). Immunostaining using a monoclonal antibody against NR3 was performed on the same Tg (*top right*) and control (*bottom right*) mice. Scale bar = 200 μm. WT, wild-type. *E* and *F*: high-powered view of EGFP expression in the hippocampal CA1 region (*E*) and cerebral cortical layer IV to VI (*F*). Scale bar = 50 μm. *G*: Western blots of the postsynaptic density fraction (PSD) from adult NR3A Tg or WT mouse forebrain. Immunoblotting was performed using anti-NR3A (*left*) or anti-PSD-95 antibody (*right*). NR3A was detected in the lane prepared from NR3A Tg but not WT control mice, while PSD-95 was equally detected in both.

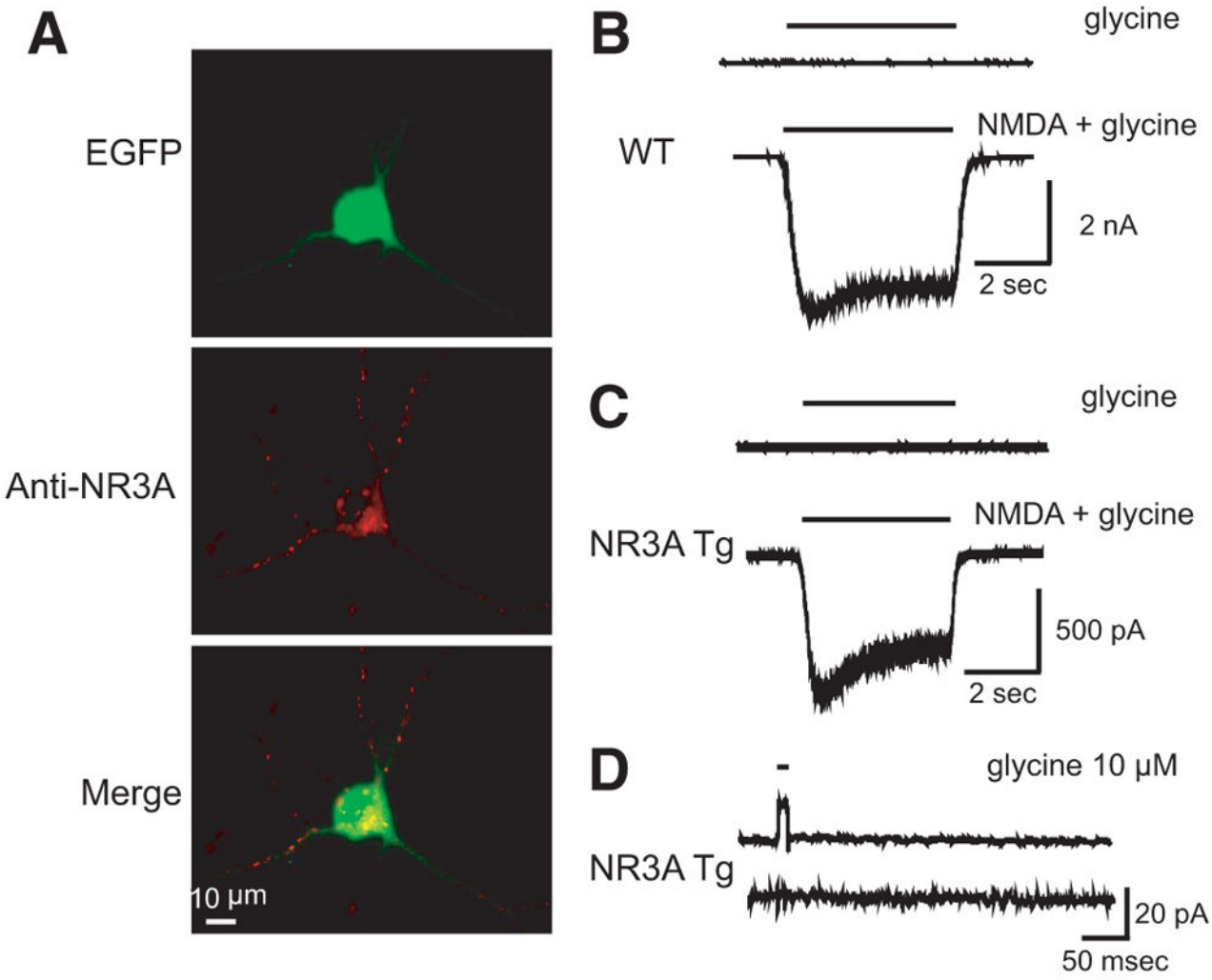

FIG. 2.

Glycine alone does not induce excitatory currents in NR3A Tg hippocampal neurons. *A*: immunohistochemistry of cultured hippocampal neurons from newborn NR3A Tg mice (14 DIV). An EGFP-positive cell (*top*) was immunostained with NR3A antibody followed by Texas Red-conjugated secondary antibody (*middle*). *B* and *C*: representative traces show that no currents were induced by application of 10 μM glycine alone in WT (*B*) or NR3A Tg neurons (*C*) (10–14 DIV). Application of 200 μM *N*-methyl-D-aspartate (NMDA) plus 10 μM glycine induced large inward currents from the same cells. *D*: representative traces after application of 10 μM glycine to an outside-out patch from an NR3A Tg neuron. The upper trace is the open-tip current recorded after patch breakdown. Holding potential, −60 mV.

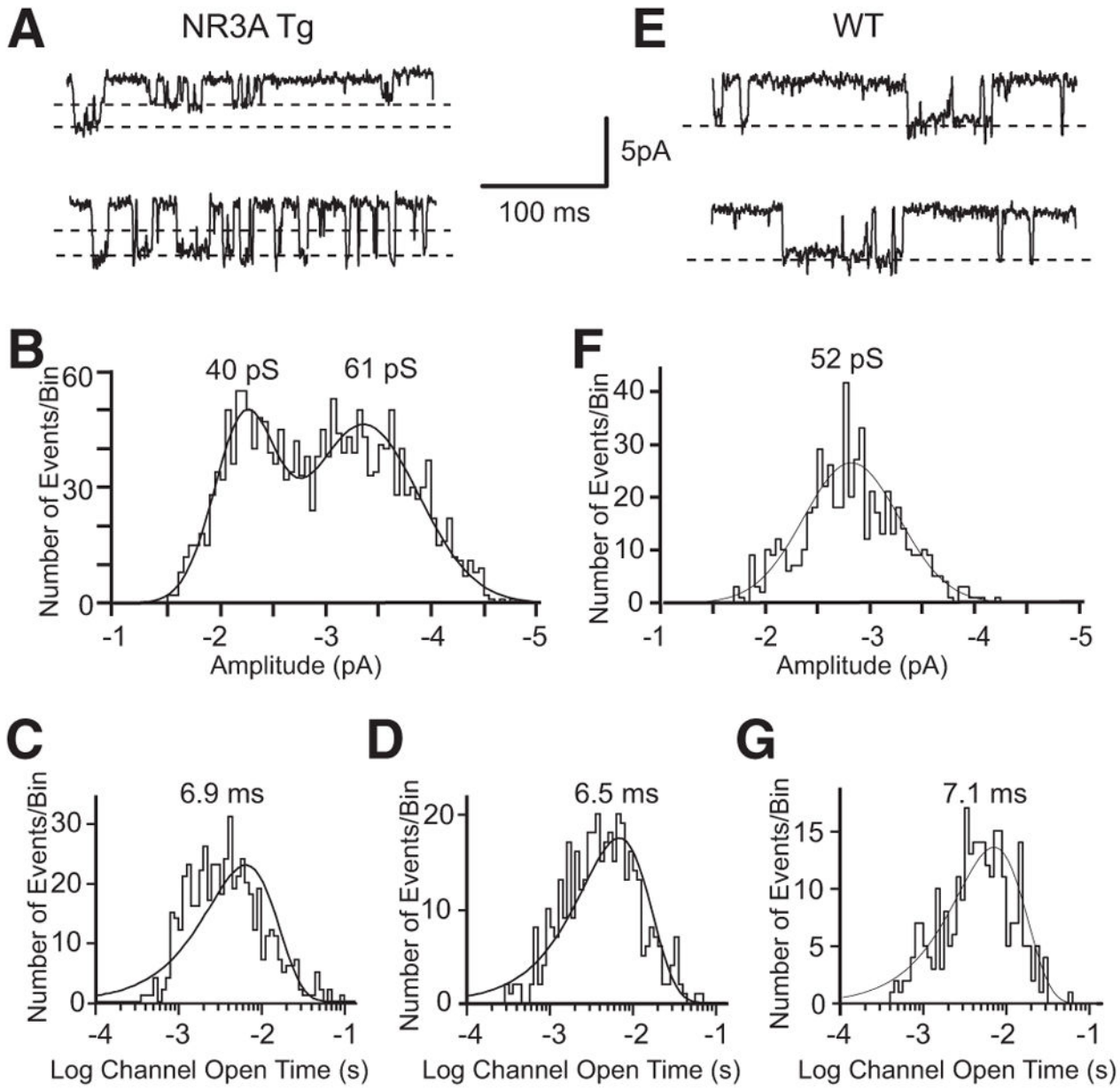

FIG. 3.

Two types of NMDA receptor (NMDAR)-operated channels in NR3A Tg neurons. *A* and *E*: representative single-channel openings at a holding potential of −55 mV induced by application of 10 μM NMDA plus 20 μM glycine in NR3A Tg neurons (*A*) and WT neurons (*E*). Two distinct unitary conductance levels were observed in NR3A Tg neurons but only 1 conductance was observed in WT neurons. *B* and *F*: amplitude histograms of single-channel conductance from NR3A Tg (*B*, n = 6, total 1873 events) and WT patches (*F*, n = 4, total 559 events). *C* and *D*: open-time histograms of the large conductance (*C*) and the small conductance (*D*) from NR3A Tg neurons. The open-time histogram was best fit with 1 exponential component with an apparent mean open time of 6.9 ms for the large conductance and 6.5 ms for the small conductance channels. *G*: open-time histogram for WT

patches. The open-time histogram was best fit with 1 exponential component with an apparent mean open time of 7.1 ms.

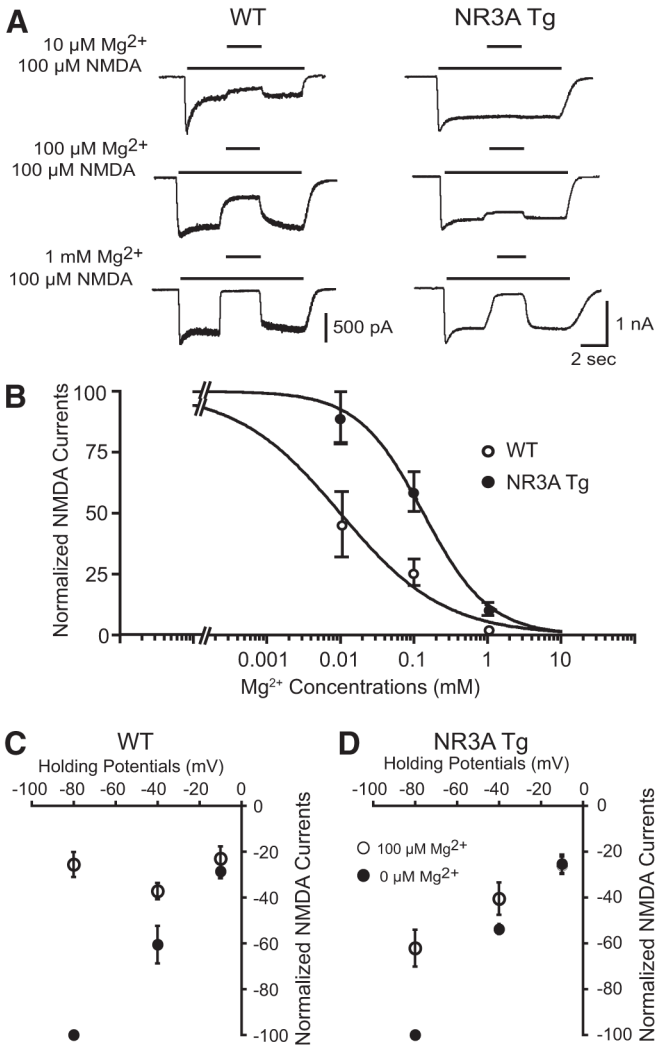

FIG. 4.

NR3A Tg neurons express NMDARs with reduced Mg^{2+} sensitivity. *A*: representative traces show blockade of NMDA currents at various concentrations of extracellular Mg^{2+} in cultured hippocampal neurons from WT (*left*) and NR3A Tg (*right*) mice. Whole cell currents were recorded in the presence of 100 μM NMDA and 10 μM glycine at a holding potential of −80 mV. *B*: dose-response curve of NMDA currents in the presence of various extracellular Mg^{2+} concentrations in WT (n = 7) and NR3A Tg neurons (NR3A Tg, n = 7) at a holding potential of −80 mV (**P < 0.01 by Student's t-test). IC_{50} values were obtained by fitting dose-response curves using the Marquardt-Levenberg algorithm with the following empirical Hill equation: $Y(\%) = 100 - \{Y_{max}/([1+(IC_{50}/[Mg^{2+}])^n]\}$, where n is the empirical Hill coefficient and IC_{50} is the apparent 50% inhibition constant. *C* and *D*: normalized NMDAR currents plotted as a function of holding potential in WT (*C*) and NR3A Tg neurons (*D*) in the absence (●) and presence (○) of 100 μMMg^{2+}. For each cell, NMDA-evoked currents were normalized to the value obtained at −80 mV in the absence of extracellular Mg^{2+}. Each data point represents the mean ± SE of responses obtained from n = 7 cells.

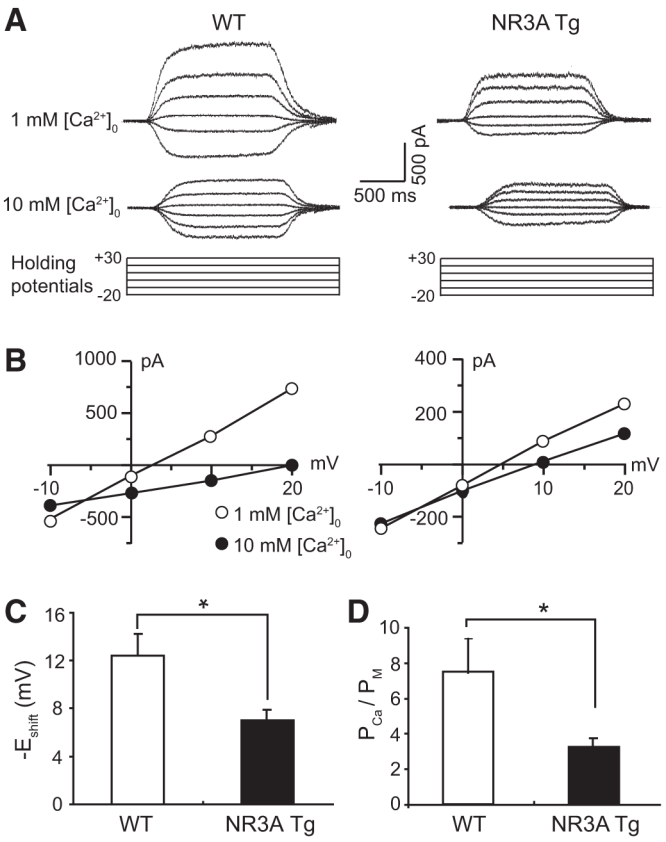

FIG. 5.

NR3A Tg neurons express NMDARs with reduced Ca^{2+} permeability. *A*: representative traces of NMDA-evoked currents (100 μM NMDA, 10 μM glycine, no added Mg^{2+}) in the presence of 1 or 10 mM extracellular Ca^{2+} from a WT (*left*) and NR3A Tg neuron (*right*) at various holding potentials. These recordings were used to calculate the reversal potential, as shown in *B*. *B*: the shift in reversal potential observed with an increase in Ca^{2+} from 1 to 10 mM was smaller in NR3A Tg neurons (NR3A Tg, *right*) than in WT neurons (WT, *left*). *C*: mean reversal potential shift in WT (n = 5) and NR3A Tg (n = 6) neurons. *D*: mean Ca^{2+} permeability ratio in WT (n = 5) and NR3A Tg neurons (n = 6; *P < 0.02 by Student's t-test).

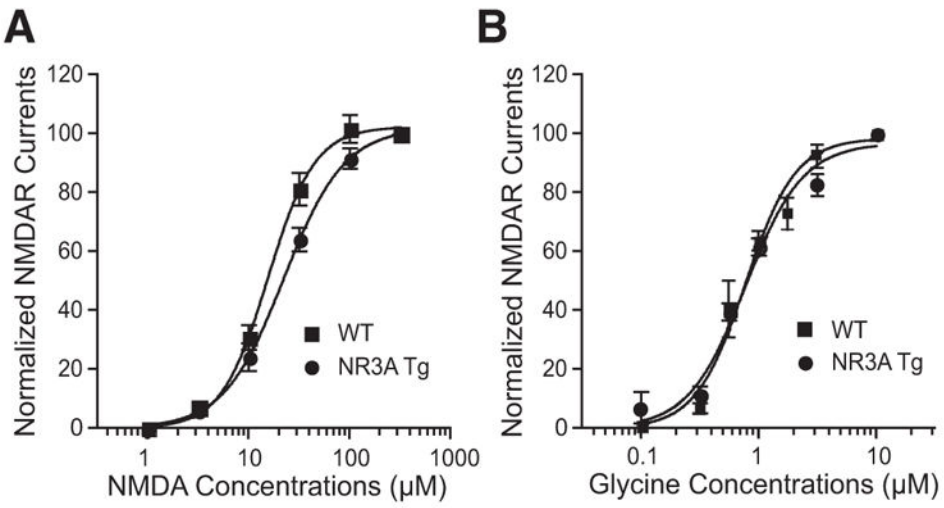

FIG. 6.

Glutamate and glycine potency remain unchanged in NR3A Tg neurons compared with WT neurons. *A*: dose-response curve for NMDA-induced currents. Whole cell currents were recorded in the presence of 10 μM glycine and various concentrations of NMDA (1–300 μM, $n = 5$; holding potential, −70 mV). *B*: glycine dose-response curve. Whole cell currents were recorded in the presence of 100 μM NMDA and various concentrations of glycine (0.1–10 μM, $n = 4 – 8$ for each data point). EC_{50} values were obtained by fitting dose-response curves with least squares to the logistic equation: $I = I_{max}/[I + (EC_{50}/[dose])^n]$, where n is the empirical Hill coefficient and [dose] represents the concentration of agonist (calculated with GraphPad Prism version 4.0c for the Macintosh; GraphPad Software, San Diego, CA, http://graphpad.com).

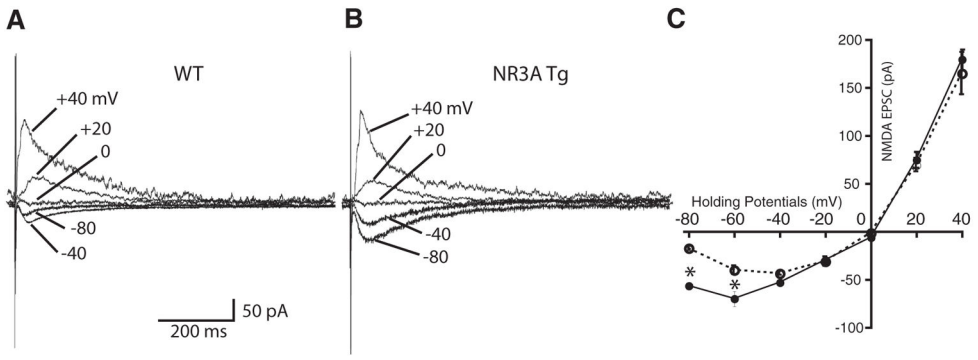

FIG. 7.

Synaptic NMDARs of NR3A Tg neurons manifest decreased Mg^{2+} sensitivity. NMDAR EPSCs were recorded at a holding potential of +40, +20, 0, −20, −40, −60, and −80 mV in the presence of 1 mM extracellular Mg^{2+}, 30 μM bicuculline (to block $GABA_A$ receptors), and 10 μM 6,7-dinitroquinoxaline-2,3 (DNQX) (to block non-NMDA receptors). *A* and *B*: representative traces show Mg^{2+} sensitivity of NMDAR-mediated EPSCs from a WT (*A*) and NR3A Tg neuron (*B*). Only 5 traces were shown for each cell for clarity. *C: I–V* curves for NMDAR excitatory postsynaptic currents (EPSCs) from WT and NR3A Tg mice (error bars indicate SE). The mean NMDAR EPSC amplitude from NR3A Tg mice was significantly greater than that from WT mice at both −60 and −80 mV (*$P < 0.01$ by *t*-test), suggesting that NR3A Tg neurons are less sensitive to Mg^{2+} blockade than WT neurons.

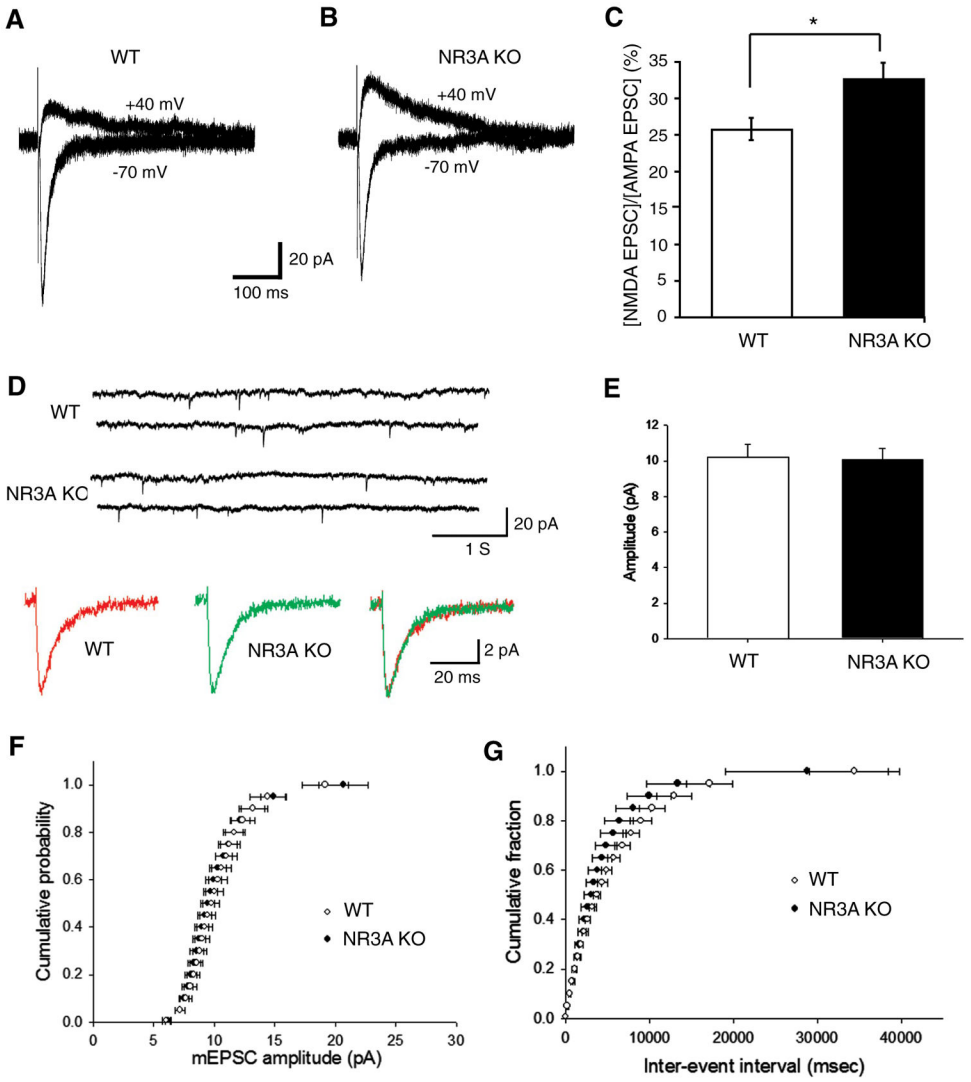

FIG. 8.

Ratio of the amplitude of NMDAR EPSCs to AMPA receptor (AMPAR) EPSCs increases in NR3A knockout (KO) compared with WT mice. *A* and *B*: representative evoked EPSCs mediated by NMDARs (at +40 mV) and AMPARs (at −70 mV) in WT (*A*) and NR3A KO (*B*) neurons. NMDA and AMPA EPSCs were recorded at a holding potential of +40 and −70 mV, respectively, in the presence of 1 mM extracellular Mg^{2+} and 30 μM bicuculline for the reasons explained in METHODS. Recordings represent mean of 4 – 8 traces. *C*: comparison of the ratio of the amplitudes of NMDAR EPSCs (amplitude measured ~50 ms after response at +40 mV) to AMPAR EPSCs (peak response obtained at −70 mV) shows that the value in NR3A KO neurons is significantly larger than that of WT neurons (*$P < 0.05$ by *t*-test). *D*: representative AMPAR mEPSCs from layer V neurons in cortical slices from NR3A KO and WT mice. *E*: mean mEPSC amplitudes from NR3A KO and WT mice. There is no significant difference between WT and NR3A KO mice ($P > 0.05$ by *t*-test). *F*: cumulative amplitude histograms are plotted from neurons of WT mice ($n = 7$ cells; 120 events/cell) and NR3A KO mice ($n = 9$ cells; 120 events/cell). There is no significant

difference between WT and NR3A KO mice ($P > 0.05$ by Kolmogorov-Smirnov test). *G*: cumulative interevent interval histograms are plotted from WT and NR3A KO neurons. There is no significant difference between WT and NR3A KO mice ($P > 0.05$ by Kolmogorov-Smirnov test).